SSRG International Journal of Electrical and Electronics Engineering
ISSN: 2348-8379/ https://doi.org/10.14445/23488379/IJEEE-V11I6P128

Volume 11 Issue 6, 259-266, June 2024

Original Article

Fabrication and Characterization of Perovskite Solar Cell with Fluorine Doped Electron Transport Layer

Sweta[1*], Laxmikant Prasad Purohit[1], Nitin Kumar Sharma[2], Hitender Kumar Malik[3], Vinod Kumar[4]

[1]*Department of Physics, Gurukul Kangri (Deemed to be University), Uttarakhand, India.*
[2]*Department of Applied Sciences & Humanities, Ajay Kumar Garg Engineering College, Uttar Pradesh, India.*
[3]*Department of Physics, IIT Delhi, New Delhi, India.*
[4]*Department of Physics, The University of the West Indies, Trinidad and Tobago, West Indies.*

**Corresponding Author : shwetasharmaphy@gmail.com*

Received: 13 April 2024 Revised: 15 May 2024 Accepted: 13 June 2024 Published: 29 June 2024

Abstract *- In today's world, the utilization of clean energy has become imperative, to meet this demand, humanity has long tapped into inexhaustible energy resources. Among these, harnessing energy from solar radiation through solar cells stands out as a prominent example. Regarding solar energy, Perovskite Solar Cells (PSCs) devices have been a revolution in this field. The reason behind their popularity is their performance. In just ten years, their performance efficiency increased at a quick pace. In comparison to traditional silicon-based Solar Cells (SC), PSCs have higher tunability and lower fabrication costs. PSCs can be constructed using either n-i-p or p-i-n configurations. Here, 'n' stands for 'Electron Transport Layer (ETL)', 'p' stands for 'Hole Transport Layer (HTL)', and 'i' shows the active material layer, which is positioned between the ETL and HTL. In the current study, TiO_2 is employed as the ETL, NiO serves as the HTL, and perovskite is utilized as the active layer. Here, titanium tetra isopropoxide precursor solution serves the purpose in the investigation for developing films of unadulterated TiO_2 and F - TiO_2 using the sol-gel followed by a spin coating process, different concentrations of F-doped TiO_2. The produced film is characterized using a range of techniques, including XRD and SEM, to ascertain its structural properties and surface morphology. The electrical properties were evaluated to determine the current density and voltage using a solar simulator, which subsequently facilitated the calculation of device performance. XRD analysis confirmed the crystalline nature and particle size. Scanning Electron Microscopy SEM images revealed distinct layers, clearly indicating proper deposition of all layers. Electrical measurements demonstrated that the concentration of fluorine doping significantly affects the performance of the device. The PCE (Power Conversion Efficiency) of the fluorine-doped samples is much more impressive than that of the un-adulterated samples in the context of the obtained results.*

Keywords *- Sol-gel, AC conductivity, Power conversion efficiency, Perovskite Solar Cell, Renewable energy.*

1. Introduction

In the battle against climate change, the capacity to produce electricity from sources of clean energy is crucial. Since the sun emits four million exa-joules (EJ =10^{18} joules) of Solar Radiation (SR) onto Earth's surface each year, the incidence of SR on the surface of Earth is sometimes considered the ideal plentiful, even environmentally friendly source of energy [1, 2]. As an illustration of its significance, more energy is delivered to Earth in an hour of sunshine than is utilized within a year [3].

Solar cells, which are gaining popularity as renewable energy sources, require characteristics of stability, excellent performance, and cheap cost. Silicon Solar Cell (SC) systems have exceptional stability and performance near their theoretical limit. Nonetheless, applying these cells to electronics, apparel, and building materials with many curves and transparent properties is problematic. Organic SC and dye-sensitized SC were examined to address this. But still, limits concerning stability, efficiency, and durability persist. The Perovskite Solar Cells' (PSCs') Power Conversion Efficiency (PCE) has been found to improve dramatically; it was 3.8% in 2009, and now, from a recent report, it is 25.8% [4]. This is explained by the materials' enormous large charge-carrying diffusion length, low exciton-binding energy, high mobility, and absorption coefficient [5].

Unfortunately, perovskite compounds are hygroscopic; therefore, they react quite strongly to humidity. Organic components [6], therefore one of the biggest obstacles in production and sustainability for a long time in the surrounding atmosphere, are identified for potential large-scale use in the future [7]. Perovskites feature a crystal

structure defined by the formula ABX_3, where A is an organic cation such as Methyl-Ammonium (MA^+), and B is a metal like lead (Pb) or other divalent metal from group 14 and represents a halogen, e.g. iodine (I), chlorine (Cl) etc.

The association between the A and X in this configuration creates a three-dimensional chemical system. In various device architectures, perovskite (i) is placed between distinct positive (p) and negative (n) contact materials. This results in two primary solar cell configurations: p-i-n (inverted) and n-i-p (planar), with the perovskite absorbing light intrinsically as a semiconductor. The accompanying Figure 1 illustrates the perovskite crystal structure.

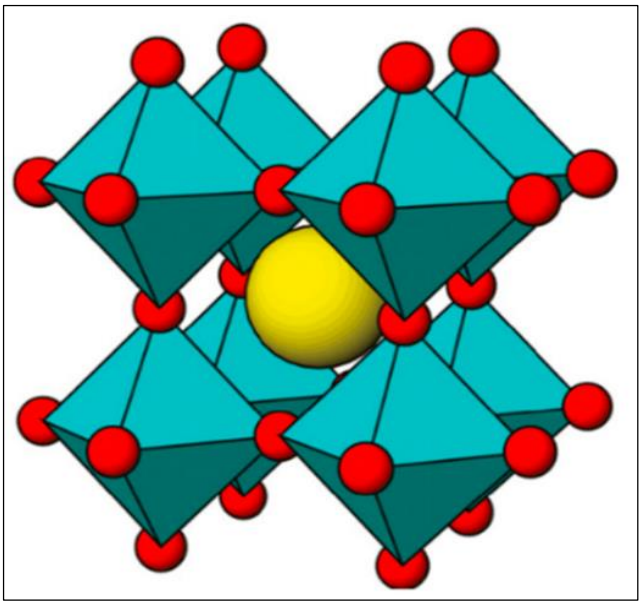

Fig. 1 Schematic image of perovskite crystal [4]

It has been documented that the modification of the perovskite material's properties can be achieved through various substitutions aimed at adjusting the bandgap and enhancing its stability against degradation. These substitutions encompass the incorporation of alternative halides, like bromine (Br) and chlorine (Cl), resulting in the formation of $MAPbBr_3$ (methyl-ammonium lead bromide) and $MAPbCl_3$ (methyl-ammonium lead chloride)

Additionally, composite structures can be synthesized by precisely mixing different halogen species, leading to the creation of compounds such as MAPb(I1-xBrx)3 and MAPb(I1-xClx)3 [8]. After the discovery of perovskite material, much research has been done, resulting in a significant increase in its power conversion efficiency. Furthermore, much improvement is expected in the upcoming years, as illustrated in the following Figure 2. The market capital for PSCs is also expected to rise with great potential in the upcoming years, as shown in Figure 3.

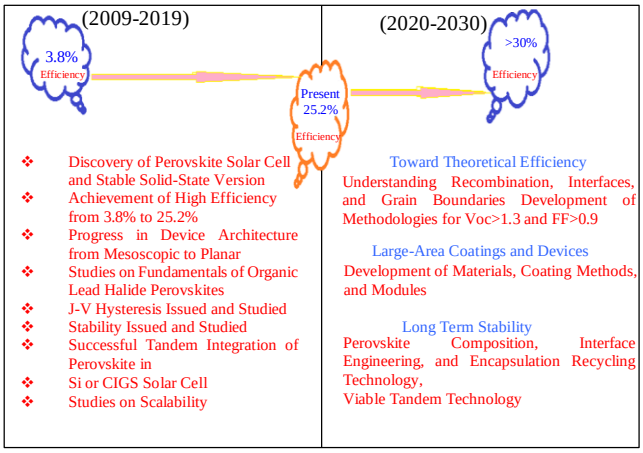

Fig. 2 Research impact in PSCs (Park, N. G. (2019). Perovskite solar cell: research direction for next ten years.

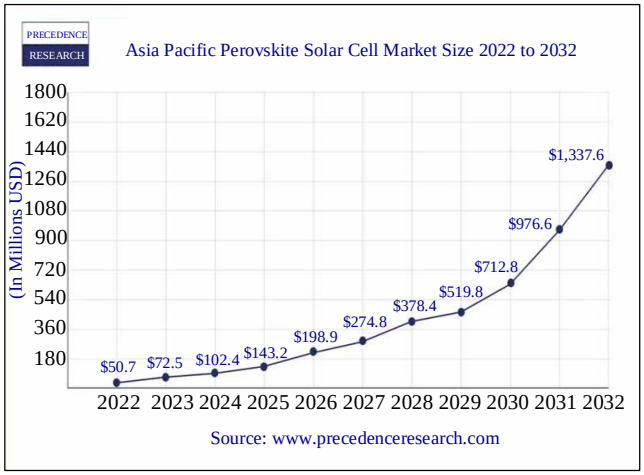

Fig. 3 The market size till 2032

The stability of PSCs in the surrounding atmosphere can be increased through the widespread application of interface engineering and encapsulation technology, which has clear benefits [9]. Most teams prepare PSCs inside a glove box filled with N_2 so that moisture cannot enter the room while the devices are being made. Additionally, a number of research teams found that the crystalline structure was very poor for resultant perovskite films when the films were synthesized in a glovebox under an inert atmosphere. However, upon exposure to specialized humidity-regulated conditions, very fast crystallization was noted [10]. Nonetheless, the most effective option for mass manufacturing in the future is to easily build highly efficient PSCs in the surrounding atmosphere that is, without the need for a glove box or a specially designed humid environment. Techniques for developing air-processed PSCs have recently been developed, and they can be broadly categorized into two categories:

1. Developing novel and straightforward manufacturing techniques to produce outstanding perovskite films that can be processed in normal surrounding conditions.

2. Investigating new perovskite compounds with essentially strong air stability. Preheating substrates have been used in the initial approach as an easy and efficient way to manufacture PSCs at room temperature. After preheating substrates to 200 °C, one group documented the highest PCE was 7.9%, while spin-coating perovskite films in the surrounding atmosphere in a single step [11]. The second method involves fabricating inorganic PSCs based on $CsPbBr_3$ in the surrounding atmosphere, resulting in the greatest level of PCE (7.78%) [12].

In addition, Tai et al manufactured PSC in an open atmosphere with the use of lead (II) thiocyanate precursor rather than PbI_2, which was very efficient and stable. After computing the device parameters, it was found that the devices showed maximum values of 15% and average PCEs of over 13% [13]. The authors did not, however, thoroughly examine the part humidity plays in the crystallization of PbI_2 films and their transformation into perovskite films. The PCE is still low and rarely rises over the documented 16%, even after multiple groups have attempted to synthesize the PSCs device in the surrounding atmosphere [6]. Following the synthesis of fluorine doped n-type TiO_2 films using the sol-gel spin coating technique - for which there are no published works - conventional n-i-p structured PSCs were manufactured using both undoped as well as doped n-layers. XDR, SEM, and other characterization techniques were used to assess the freshly manufactured devices.

1.1. How a Solar Cell does Work

Employing the material known as semiconductors, the limitless resources can be revolutionized into electricity by the photovoltaic effect [14]. Figure 4 reveals that the general functioning principle involves using electromagnetic radiation from the sun to move a valence band electron towards a conduction band. The bandgap, which is the energy imbalance between the conduction and valance bands, is a distinctive feature of semiconductor materials. As a result, electron-hole pairs are formed, and a flow of electricity is produced if the excited electrons are returned to the valence band via an external circuit [15] (see Figure 6b).

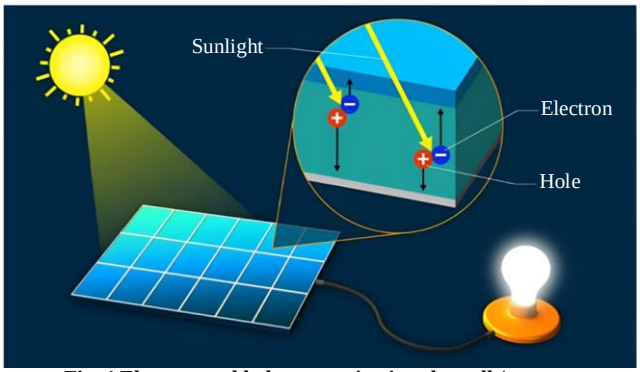

Fig. 4 Electron and hole generation in solar cell (source: https://glsolarpower.com/construction-and-working-principle-of-silicon-solar-cells/)

2. Materials and Methods

Titanium Tetra Isopropoxide (TTIP), trifluoroacetic acid as a source of Ti and F, respectively and 2-methoxy ethanol, lead iodide, and methylamine hydroiodide were bought from Sigma-Aldrich. The water utilized during the experiment was Deionized (DI). No additional purification was done in the chemicals; all of the compounds were analytical grade when they were applied.

2.1. Preparation of n-Type of TiO_2 Layer

Several films were prepared with two types of TiO2: pure and fluorine-doped via sol-gel, followed by a spin coating technique [16]. Chemically and thermally stable films of TiO_2 were deposited using the spin coating technique.

For thin film deposition, a substrate made of Fluorine-doped Tin Oxide (FTO) was utilized, and it was properly cleaned. The detergent washed the substrate then ultra-sonicated and finally dried. The precursor solutions were prepared by using TTIP and tri fluoro acetic acid as a source of F, respectively, while 2 methoxy ethanol was used as a solvent.

The F-doped TiO_2 solutions 0 2 4 6 8 at % were prepared separately and stirred 120 min at room temperature. After getting transparent homogeneous solutions then all solutions were kept for ageing for 24 h to accomplish all chemical reactions between them. Before the deposition, all solutions were filtered and then coated the thin films over the surface of the substrate at a constant rate of 2500 rate per minute (r.p.m.) for 30 sec.

Further, after each deposition, thin films were dried at a temperature of 200 °C for 10 min, in a muffle furnace; same procedure was repeated 10 times. Thus, the resulting thin film was annealed for 60 minutes at 450 °C in a muffle furnace.

2.2. Preparation of Perovskite Layer

Various researchers have prepared perovskite layers via spin coating using a one-step deposition method or by single-step deposition [17]. In 0.63 mL of DMF, 461.0 mg of PbI_2, 159.0 mg of CH_3NH_3I, and 72.0 mg of DMSO were dissolved to create the perovskite precursor solution. The resultant mixture was spin-coated for 30 seconds at 2500 rpm after being agitated for two hours at 80 °C.

2.3. Preparation of Nickel Oxide (NiO HTL) Layer

Various researchers have worked with nickel oxide in solar cells to make the p-type or HTL layers [18, 19]. 0.24 gm The 9.85 ml of DI was mixed with nickel acetate and agitated. NaOH is added dropwise till no further precipitation stops.

The formed precipitate is centrifuged and cleaned 3 times using DI. The obtained solution is dried at 100°C for 2 hr. After drying, the obtained compound is annealed at 300 ˚C for 5 min to form NiO nanoparticles.

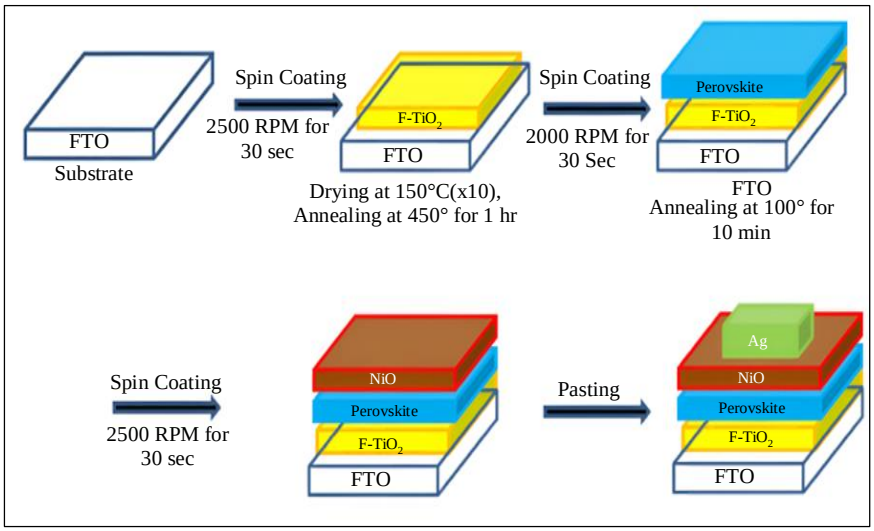

Fig. 5 Steps for fabrication of PSC

2.3.1. NiO HTL Deposition

NiO HTL solution is prepared by adding NiO nanoparticles in isopropanol (2% wt.). Then, the solution was spin-coated over perovskite film via a one-step deposition technique at 2500 r.p.m. for 30 sec. After the deposition of NiO, Ag contact was made. By following all these steps f-doped TiO_2 perovskite solar cell was Synthesized, followed by the NiO layer. The structure of the device is n-i-p.

2.4. Process of Fabrication of Device

Figure 5 shows the step of deposition of layers for the device fabrication.

3. Characterization

The sample's X-Ray Diffraction (XRD) pattern was obtained by diffractometer over an extensive range of 10° to 80° on a 2θ scale. The CuKα wavelength of the monochromatic light in the XRD diffractometer is 1.54Å at 40 kV at a rate of 6°/min. To assess the layers deposited, Scanning Electron Microscopy (SEM) was employed. Under AM 1.5 sun intensity, current-density vs voltage curve (J-V) were measured using an instrument, Keithley 2400 source table and a light source of 450 W (Xenon- lamp). For Photoluminescence measurement, Perkin Elmer (model no. LS55) was used.

4. Results and Discussion

PSC structures are displayed in Figure 6 (a), and the energy band for the device components is displayed in Figure. 6(b). The device was successfully manufactured under the glove box and ambient conditions. FTO was used as a substrate and an electrode in PSCs, and Ag was pasted to fabricate the opposite electrode. Because NiO has good hole mobility and TiO_2 layers have high electron mobility, here TiO_2 in pure and doped form severs the purpose Electron Transport Layer (ETL), and NiO was deposited to make a layer of Hole Transport Layer (HTL).

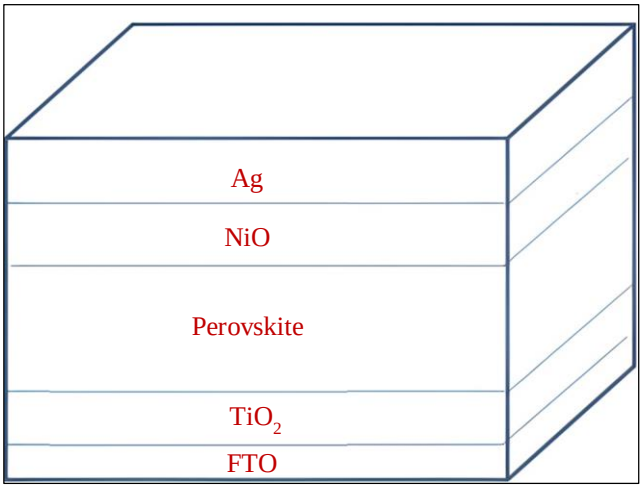

(a)

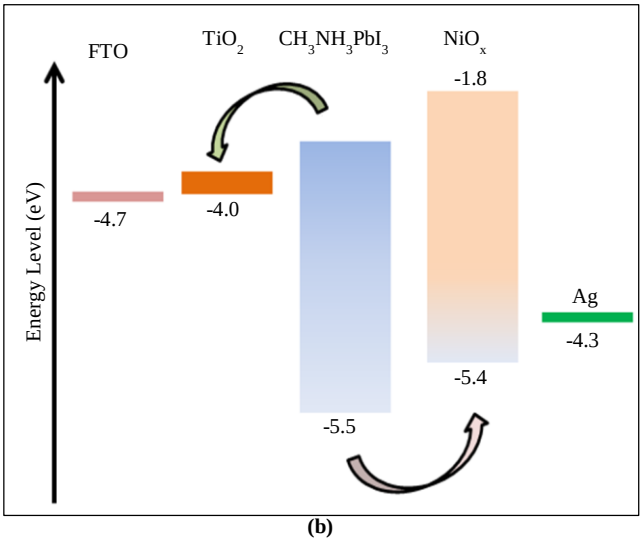

(b)

Fig. 6(a) Displaying the structure of the device, and (b) Energy band diagram for the device structure.

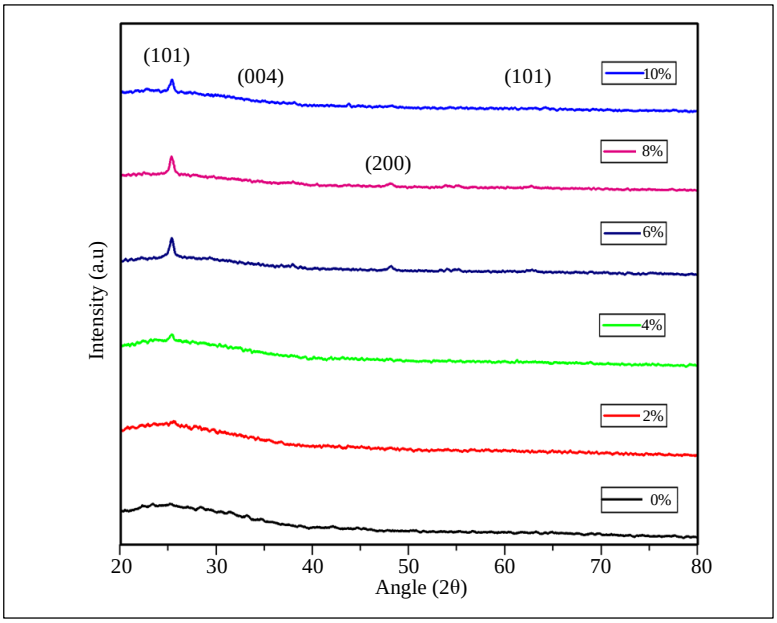

Fig. 7 XRD pattern of pristine TiO_2 and F-doped TiO_2

4.1. X-Ray Diffraction (XRD) Analysis

Among the most significant for examining the sample's crystallinity and structure is XRD. The patterns are shown for all the samples in Figure 7, which were confirmed by references in the literature. The crystal structure of TiO_2 was confirmed with XRD and also verified with JCPDS Card no. 21-1272, and peaks were found at the angles of 24.8°, 37.3°, and 47.6°; they match with planes (101), (004), and (200). The peaks of each pattern fit the anatase TiO_2 lattice planes [20].

Furthermore, as the doping concentration rises, certain peaks that correspond to fluorine (101) become more noticeable in the pattern. The average grain size, or crystallite size, was calculated using the Scherrer formula and can be seen in Equation (1) [21]. The equation was derived for the ideal condition in which monodisperse powder, which is monochromatic, infinitely narrow, and perfectly parallel cube-shaped crystallites, was used. The Equation can be written as,

$$D_{hkl} = K\lambda/(B_{hkl}\cos\theta) \quad (1)$$

Here, D represents crystallite size, hkl are miller indices of the planes being investigated, K is a numerical value considered as the crystallite-shape factor, which also depends on crystal size, λ is a symbol of wavelength here represents the wavelength of X-ray, and B symbolizes FWHM (Full-Width at Half-Maximum) of the X-ray diffraction peak in radians, and θ is the Bragg angle.

This method is generally accepted to calculate the average sizes of particles, and the size of particles ranged between less than 35 nm. The result is summarized in Table 1. It proves that the fluorine doping modifies TiO_2 particle size marginally.

Table 1. The crystal size for different doping concentrations

Doping (%)	Crystal Size/Grain Size (nm)
0	29.43
2	31.74
4	30.89
6	31.22
8	31.86
10	28.29

4.2. Surface Morphology

The physical structure of the prepared devices was analyzed with Scanning Electron Microscopy (SEM). Figures 8 and 9 display the SEM images of prepared devices, respectively, at various levels of magnification. SEM images show that at higher magnifications, one can observe miscible surface morphology characterized by a compact structure with few pinholes and layer separation, which are also demonstrated in Figure 8 (a-d) and Figure 9 (a-b).

Here, Figure 8 (a) confirms the layer deposition for the device and (b and c show the thickness of layers). In Figure 9 (a and b), NiO has formed a cluster. This can be due to moisture, and also NiO tends to form clusters due to its high surface area energy [22].

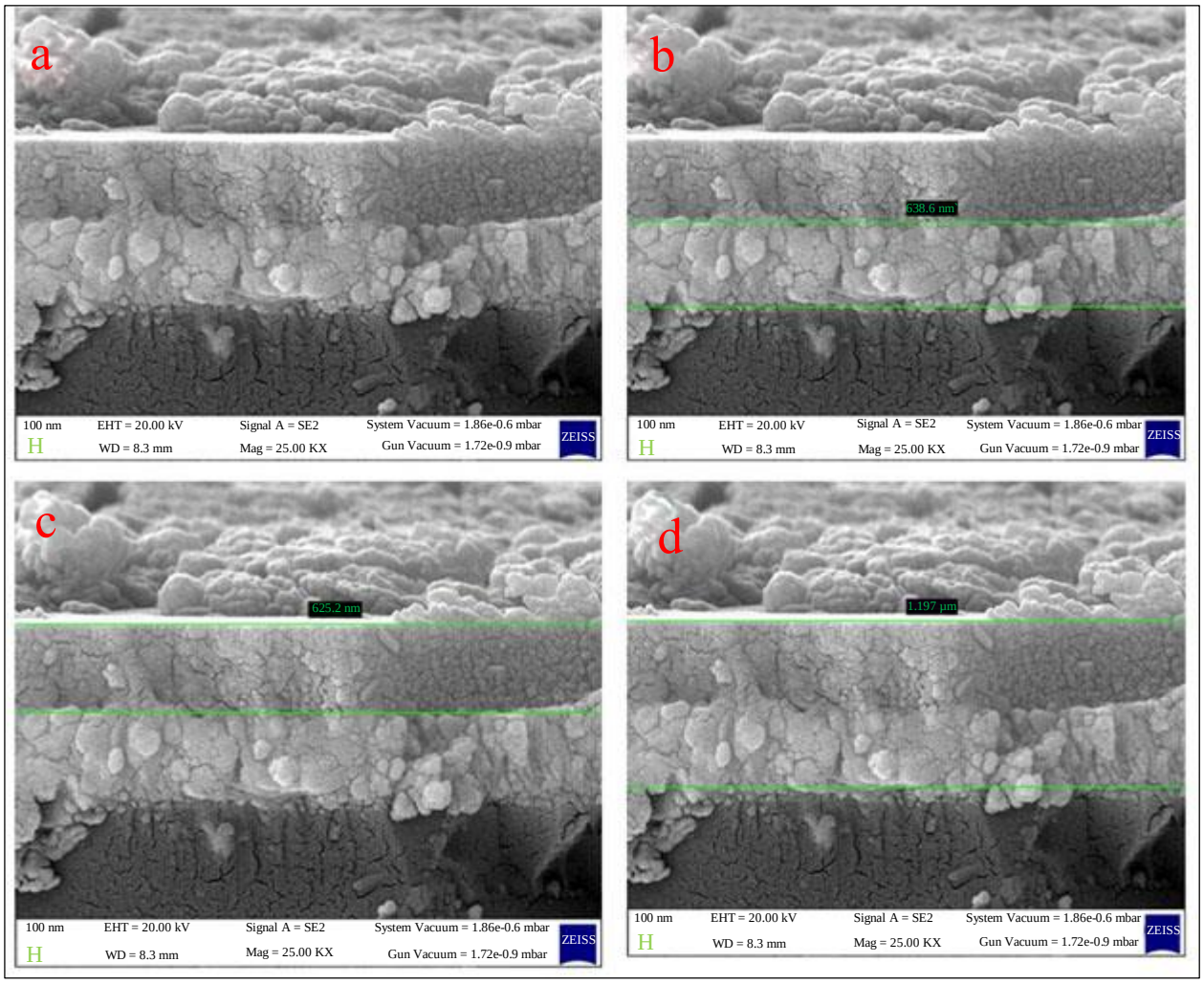

Fig. 8 SEM images of (a) n-i-p (TiO_2/perovskite/NiO), (b) Width of perovskite layer, (c) Width of NiO layer, and (d) Thickness of perovskite and NiO layer

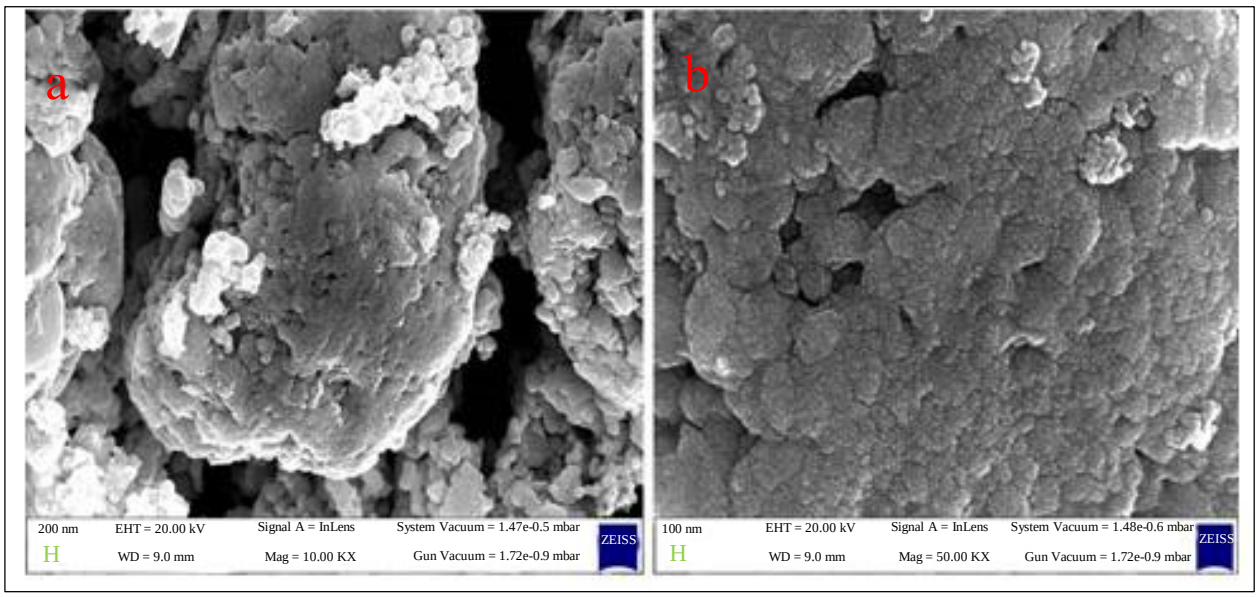

Fig. 9 Images from SEM of NiO layer (a and b) top view of NiO layer at different magnifications

4.3. Power Conversion Efficiency

What effects does the fluorine doping of TiO_2 have on the properties of PSCs? The J-V curves (Figure 10) show that the same technique was employed to manufacture the mesoporous layer and generate the PSC with various TiO_2 samples. All of the PSCs were then examined under light intensities that were similar to AM1.5. The associated parameters are given in Table 2. It appears that the PCE calculated using an undoped sample (0%) is 2.33%, but PCE, based on doped samples (2-6%), is much improved. The greatest value of the PCE, which is based on a 6% doped sample, is 5.83%. The PCE of the 8% doped sample decreases. This may be due to an excessive amount of fluorine. Fluorine peaks are clearly visible in the 8% doped XRD pattern (Figure 7). Consequently, excess fluorine deposited on the surface of the TiO_2 grain reduces the PCE, preventing photoelectron transmission between TiO_2 grains.

Table 2. Device parameters F- doped and undoped samples

Doping Concentration	J_{sc}(mA/cm^2)	V_{oc}(V)	FF	PCE (%)
0	19.97	0.96	0.31	2.33
2	20.56	0.96	0.36	3.29
4	20.96	0.98	0.39	5.22
6	23.27	1.02	0.42	5.83
8	21.76	0.98	0.28	2.12

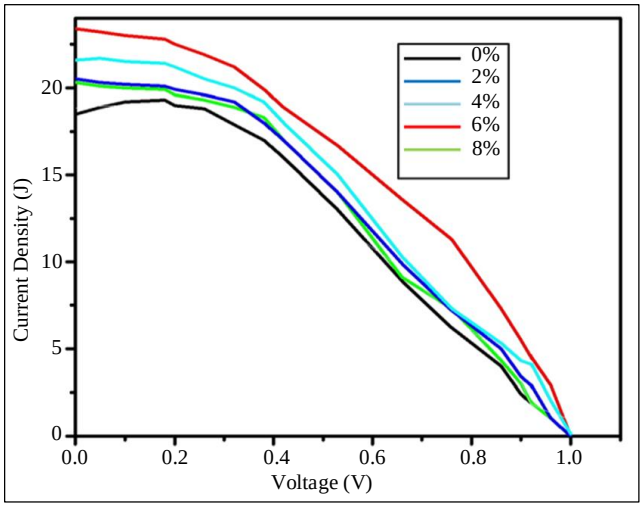

Fig. 10 Voltage Vs current density (V Vs J-V) for perovskite solar cell

The Photoluminescence (PL) was performed on a number of TiO_2/perovskite/NiO films to confirm that fluorine doping improves TiO_2 electron transport and propels the PCE's boost. The outcomes are displayed in Figure 11. The prominent peak is seen in all PL spectra at approximately 335 nm, which agrees with previous investigations [23]. The order of the peak intensity is 6%> 8% > 0%, according to the J-V result above, demonstrating the effectiveness of photo-generated electrons and their extraction and transport.

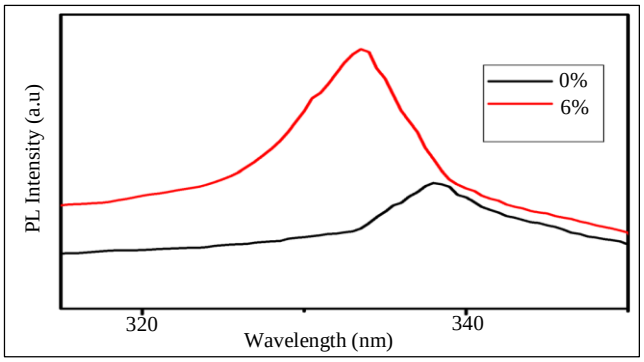

Fig. 11Wavelength vs PL intensity

5. Conclusion

According to an X-ray analysis, TiO_2 exhibits crystalline domains. The dielectric constant increases with rising temperature and decreases with increasing frequency at low frequencies; at high frequencies, there is a strong frequency/temperature correlation. It seems that AC conductivity increases with frequency and decreases with temperature. On the basis of this study, it can be concluded that a limited amount of F doping can increase the PCE as the unadulterated samples showed a PCE of about 2.33%, and 6% samples showed a PCE of 5.83%, further increment in doping resulted into decrease in PCE, this can also be verified by XRD and PL results. So many researchers have done the same.

5.1. Novelty of work

The device fabrication was carried out without using a compact layer of TiO_2, as it is not essential for achieving better Power Conversion Efficiency (PCE) and helps to reduce costs [24]. Instead of organic compounds like spiro-OMeTAD or PTAA, NiO (an inorganic compound) was used as the HTL due to its reduced cost of materials, improved stability and increased carrier mobility. Organic HTLs often suffer from raised material expenses, inadequate stability and insufficient carrier mobility, significantly limiting their real-world uses [25]. Although the device demonstrated slightly lower efficiency with these materials, it remained both sustainable and highly cost-effective. This (FTO/TiO_2 /$CH_3NH_3PbI_3$ /NiO) device architecture has not been tried by any research group in our information.

5.2. Future scope

Different doping materials and concentrations can do ETL (TiO2) modifications. Some more inorganic compounds can be tried as HTL for sustainable and cost-effective PSCs.

Acknowledgment

The central instrumentation facilities of IIT Roorkee and IIT New Delhi are acknowledged for providing SEM and XRD.PL was done at the Jaypee Institute of Information and Technology. The semiconductors research lab at Gurukula Kangri (deemed to be) University is acknowledged for providing an LCR facility and Xenon lamp.

References

[1] Pabitra K. Nayak et al., "Photovoltaic Solar Cell Technologies: Analysing the State of the Art," *Nature Reviews Materials*, vol. 4, no. 4, pp. 269-285, 2019. [CrossRef] [Google Scholar] [Publisher Link]

[2] Ehsanul Kabir et al., "Solar Energy: Potential and Future Prospects," *Renewable and Sustainable Energy Reviews*," vol. 82, pp. 894-900, 2018. [CrossRef] [Google Scholar] [Publisher Link]

[3] Nathan S. Lewis, and Daniel G. Nocera, "Powering the Planet: Chemical Challenges in Solar Energy Utilization," *PNAS*, vol. 103, no. 43, pp. 15729-15735, 2006. [CrossRef] [Google Scholar] [Publisher Link]

[4] Priyanka Roy et al., "Perovskite Solar Cells: A Review of the Recent Advances," *Coatings*, vol. 12, no. 8, pp. 1-24, 2022. [CrossRef] [Google Scholar] [Publisher Link]

[5] Jian Wu et al., "Fabrication of Efficient Organic-Inorganic Perovskite Solar Cells in in Ambient Air," *Nanoscale Research Letters*, vol. 13, pp. 1-7, 2018. [CrossRef] [Google Scholar] [Publisher Link]

[6] Di Liu et al., "Tailoring Morphology and Thickness of Perovskite Layer for Flexible Perovskite Solar Cells on Plastics: The Role of CH3NH3I Concentration," *Solar Energy*, vol. 147, pp. 222-227, 2017. [CrossRef] [Google Scholar] [Publisher Link]

[7] Ningxia Gu et al., "Fabrication of Efficient and Stable Perovskite Solar Cells in Open Air through Adopting a Dye Interlayer," *Sustainable Energy & Fuels*, vol. 6, no. 18, pp. 4275-4284, 2022. [CrossRef] [Google Scholar] [Publisher Link]

[8] Hyun Suk Jung, and Nam-Gyu Park, "Perovskite Solar Cells: From Materials to Devices," *Small*, vol. 11, no. 1, pp. 10-25, 2015. [CrossRef] [Google Scholar] [Publisher Link]

[9] Enbing Bi et al., "Diffusion Engineering of Ions and Charge Carriers for Stable Efficient Perovskite Solar Cells," *Nature Communications*, vol. 8, pp. 1-7, 2017. [CrossRef] [Google Scholar] [Publisher Link]

[10] Y. Kumar et al., "Effect of Heat Treatment on the Electrical Properties of Perovskite Solar Cells," *Solar Energy Materials and Solar Cells*, vol. 157, pp. 10-17, 2016. [CrossRef] [Google Scholar] [Publisher Link]

[11] Gwang Su Shin et al., "Rapid Crystallization in Ambient Air for Planar Heterojunction Perovskite Solar Cells," *Electronic Materials Letters*, vol. 13, pp. 72-76, 2017. [CrossRef] [Google Scholar] [Publisher Link]

[12] Weijie Chen et al., "A Semitransparent Inorganic Perovskite Film for Overcoming Ultraviolet Light Instability of Organic Solar Cells and Achieving 14.03% Efficiency," *Advanced Materials*, vol. 30, no. 21, 2018. [CrossRef] [Google Scholar] [Publisher Link]

[13] Qidong Tai et al., "Efficient and Stable Perovskite Solar Cells Prepared in Ambient Air Irrespective of the Humidity," *Nature Communications*, vol. 7, pp. 1-8, 2016. [CrossRef] [Google Scholar] [Publisher Link]

[14] Paul Rappaport, "The Photovoltaic Effect and Its Utilization," *Solar Energy*, vol. 3, no. 4, pp. 8-18, 1959. [CrossRef] [Google Scholar] [Publisher Link]

[15] N.D. Kaushika, Anuradha Mishra, and Anil K. Rai, *Solar Photovoltaics - Technology, System Design, Reliability and Viability*, 1st ed., Springer Cham, 2018. [CrossRef] [Google Scholar] [Publisher Link]

[16] Ajay Sharma, R.K. Karn, and S.K. Pandiyan, "Synthesis of TiO_2 Nanoparticles by Sol-Gel Method and their Characterization," *Journal of Basic and Applied Engineering Research*, vol. 1, no. 9, pp. 1-5, 2014. [Google Scholar] [Publisher Link]

[17] Abraha Tadese Gidey et al., "First Conventional Solution Sol-Gel-Prepared Nanoporous Materials of Nickel Oxide for Efficiency Enhancing and Stability Extending MAPbI3 Inverted Perovskite Solar Cells," *ACS Applied Energy Materials*, vol. 4, no. 7, pp. 6486-6499, 2021. [CrossRef] [Google Scholar] [Publisher Link]

[18] K. Anandan, and V. Rajendran, "Morphological and Size Effects of NiO Nanoparticles via Solvothermal Process and their Optical Properties," *Materials Science in Semiconductor Processing*, vol. 14, no. 1, pp. 43-47, 2011. [CrossRef] [Google Scholar] [Publisher Link]

[19] Diego Di Girolamo et al., "Progress, Highlights and Perspectives on NiO in Perovskite Photovoltaics," *Chemical Science*, vol. 11, no. 30, pp. 7746-7759, 2020. [CrossRef] [Google Scholar] [Publisher Link]

[20] Wenjuan Li et al., "Generation of Oxygen Vacancies in Visible Light Activated One-Dimensional Iodine TiO_2 Photocatalysts," *RSC Advances*, vol. 4, no. 70, pp. 36959-36966, 2014. [CrossRef] [Google Scholar] [Publisher Link]

[21] Anand Kumar Tripathi et al., "Structural, Optical and Photoconductivity of Sn and Mn Doped TiO_2 Nanoparticles," *Journal of Alloys and Compounds*, vol. 622, pp. 37-47, 2015. [CrossRef] [Google Scholar] [Publisher Link]

[22] Sakhamudi Sai Narender et al., "Nickel Oxide Nanoparticles: A Brief Review of their Synthesis, Characterization, and Applications," *Chemical Engineering & Technology*, vol. 45, no. 3, pp. 397-409, 2022. [CrossRef] [Google Scholar] [Publisher Link]

[23] Shuangyong Sun et al., "The Origin of High Efficiency in Low-Temperature Solution-Processable Bilayer Organometal Halide Hybrid Solar Cells," *Energy & Environmental Science*, vol. 7, no. 1, pp. 399-407, 2014. [CrossRef] [Google Scholar] [Publisher Link]

[24] Dianyi Liu, Jinli Yang, and Timothy L. Kelly, "Compact Layer Free Perovskite Solar Cells with 13.5% Efficiency," *Journal of the American Chemical Society*, vol. 136, no. 49, pp. 17116-17122, 2014. [CrossRef] [Google Scholar] [Publisher Link]

[25] Cuiping Zhang et al., "A Review on Organic Hole Transport Materials for Perovskite Solar Cells: Structure, Composition and Reliability," *Materials Today*, vol. 67, pp. 518-547, 2023. [CrossRef] [Google Scholar] [Publisher Link]